ISBN: 978-3-95450-188-5 doi:10.18429/JACoW-MEDSI2016-TUCA03

ESTIMATION OF TEMPERATURE FLUCTUATIONS HARSHNESS REGARDING STABILITY OF STRUCTURES IN THE NANOMETER RANGE

N. Jobert†, F. Alves, S. Kubsky, Synchrotron SOLEIL, Saint Aubin, France

Abstract

Along with mechanical vibrations, thermal-mechanical deformations are the primary contributor to positional and pointing errors. This paper deals with specific analysis and interpretation difficulties encountered when designing and validating ultimate stability systems (i.e. in the range of a few nm). When attempting to design such systems, it is not sufficient to simply reduce overall temperature fluctuations, but it becomes necessary to target efforts at the specific components that are detrimental to the dimensional stability of the system. This calls for an integrated approach where temperature measurements, data analysis and reduction are performed in conjunction with a priori knowledge of the thermal-mechanical system behaviour.

1 INTRODUCTION

When dealing with high-accuracy devices, thermally induced distortions are a key contributor to the overall positional and pointing performance of the system. While it is both correct and obvious that the smaller the temperature fluctuations, the more stable the system will be, there is some hidden complexity in the subject.

Firstly, not all temperature fluctuations will actually distort the structure: very short period (i.e. 'fast') variations will not propagate far into the structure, and will induce very little change in overall dimensions. Nevertheless, they can induce local distortions, hence small positional errors but possibly larger pointing errors. Conversely, very long period (i.e. slow') temperatures fluctuations will result in quasi uniform temperature fields and therefore will efficiently change overall dimensions but possibly induce lower pointing errors.

Secondly, there is always some randomness in temperature fluctuations, which somehow obscures the actual severity of a given environment. This randomness occurs timewise, but also space-wise. For a highly stable environment, the random part of the temperature field has magnitude comparable or even higher to that of the general trend, and simply discarding this part becomes questionable.

Surprisingly, no harshness indicator has been developed that could help quantifying the actual severity of a given realistic thermal environment. It is the objective of this paper to provide some insight on the various phenomena at play. Additionally, we propose a simple yet efficient numerical method allowing the evaluation of actual structural responses to any realistic thermal environment. It is the wish of the authors that such approach should help in making more rational decisions, either at design or commissioning phases.

†nicolas.jobert@synchrotron-soleil.fr

2 ENGINEERING DIFFICULTIES

Thermal Mechanical Susceptibility: Intuition vs Quantitative Analysis

To illustrate the relative efficiency of various thermal fluctuations, it is instructive to start with a simple support structure: the following test-case is nearly academic, and merely aims at providing some feeling for the subject at hand. We assume an L-shaped bracket support structure which is a most desirable shape regarding vibrational stability because of its high stiffness/weight ratio along every axis (Figure 1). The engineering question is: "What about the actual thermal mechanical susceptibility of such a system?"

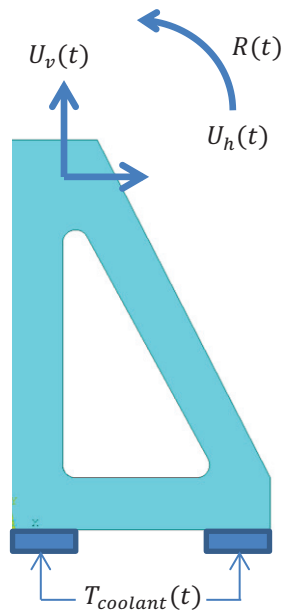

Figure 1: Academic test case.

Clearly, the answer depends on the heat path considered. Generally speaking, this can be either convection through surrounding medium (if any), radiation to the surrounding cavity, or convection to the heat sink. To further simplify the discussion, we will only consider the latter*. Also, we assume a very efficient heat transfer at bottom (which is what we aim for in real life), so that the boundary takes on nearly the same temperature as the coolant fluid.

* Note that, by principle, this is the only heat path that cannot be weakened and therefore ultimate stability will be governed by this disturbance source.

ISBN: 978-3-95450-188-5 doi:10.18429/JACoW-MEDSI2016-TUCA03

For very slow fluctuations, the temperature field in the bracket will be uniform and the displacement at support tip may be approximated using beam-type formulas:

$$\Delta U_v \sim \alpha . Height . \Delta T_{coolant} \quad (1)$$

$$\Delta U_v \sim \alpha . Width . \Delta T_{coolant} \quad (2)$$

$$\Delta R_v \sim 3/2 . \alpha . \left(\frac{Width}{Height}\right) . \Delta T_{coolant} \quad (3)$$

Now, how do we estimate what is "fast" and "slow" for such a structure? We may remember that the effective penetration depth for a harmonically time-dependent temperature imposed at the boundary of a 1D system reads:

$$\delta_{effective} \approx \sqrt{thermal\ diffusivity \times T/2\pi} \quad (4)$$

Where:

- Thermal diffusivity is defined by the material thermal conductivity, density and inertia
- T is the temperature fluctuation period

Assuming the effective penetration depth is equal to the characteristic scale of the length of the structure can give a back-of-the-envelope estimation for the boundary between "slow" and "fast" temperature fluctuations. This separation (or corner) period can read:

$$T_{corner} = \frac{2\pi L^2}{thermal\ diffusivity} \quad (5)$$

As an example, for aluminium, thermal diffusivity is about 100 mm²/s. For a 150 mm long structure (typical for optical support), this yields a separation period of about 700 s. This is consistent with engineering judgment that strongly suggests ignoring any temperature variation shorter than 10 minutes or so.

Relative Efficiency of Temperature Components

To confirm this hunch, one can build a numerical model of the structure at hand and run a series of transient thermal mechanical analyses. For each one, a harmonically time-dependent temperature is enforced at the model boundary, and the temperature / displacement in the structure can be estimated and compared to that same quantity as obtained in the static case. That procedure has been applied (using the ANSYS FEM package) to the academic test case, assuming 2D propagation, material aluminium and dimensions typical of support structure (150 mm height, 100 mm width), as shown on Figure 2.

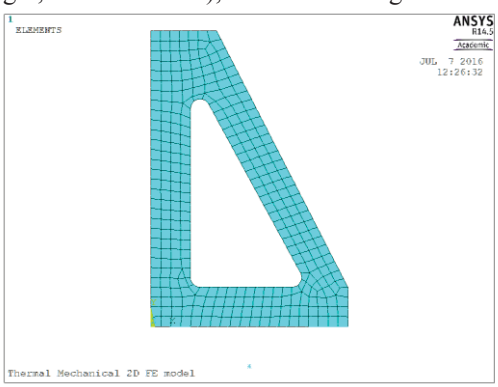

Figure 2: FEM of support structure.

The results are displayed on Figure 3 to 5 and commented hereafter.

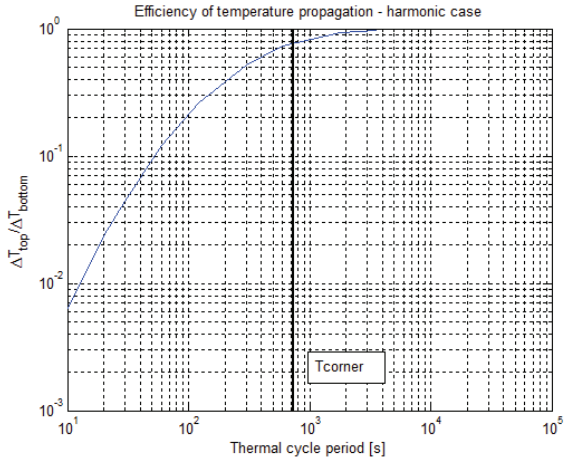

Figure 3: Relative efficiency of temperature propagation.

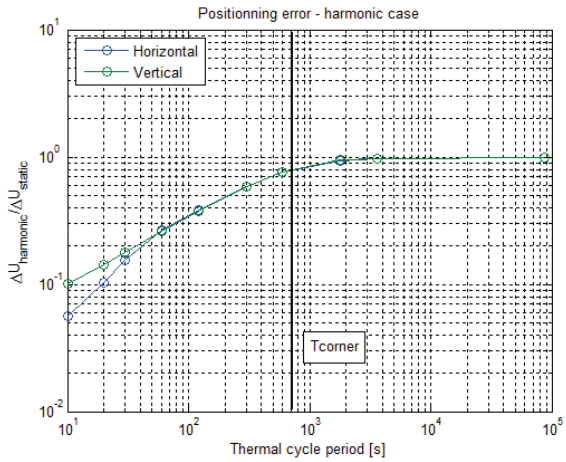

Figure 4: Relative efficiency of position error.

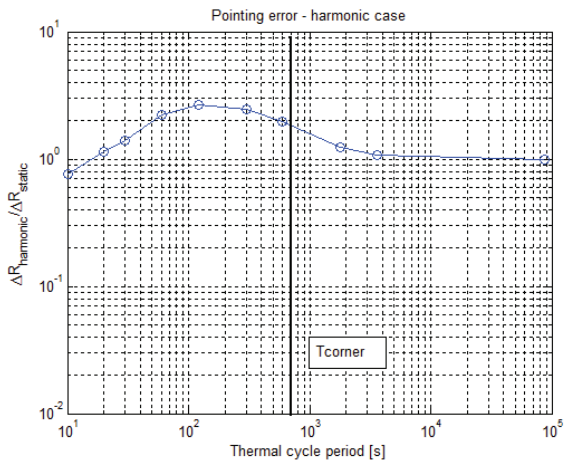

Figure 5: Relative efficiency of pointing error.

From those curves it stems that:

- temperature amplitude at structure tip decreases exponentially with decreasing period.
- positioning errors decrease as the square root of the period.
- pointing errors mildly *increase*, in the period range where the thermal wavelengths are comparable with the structural members dimensions.

ISBN: 978-3-95450-188-5 doi:10.18429/JACoW-MEDSI2016-TUCA03

Those conclusions are expected to be generic and hold true irrespective of the actual structure geometry. A practical conclusion is that, although some filtering (low-pass) effect will exist, its rejection efficiency is generally less than that suggested by intuition. Indeed, regarding dimensional stability, one gets a meagre 3dB/octave filtering effect, far from the exponential decay rate of the temperature propagation. For pointing errors, some amplification (factor 2.5 in our case) is witnessed.

Sadly enough, real-world temperature environments are rarely harmonic[†], but rather random. Therefore, when one wishes to estimate the actual severity of a given environment, an estimator for the spectral content of the temperature disturbance is needed.

3 SPECTRAL ANALYSES

Temperature Spectral Estimator

Now that we have defined the frequency-dependent susceptibility of our structure, we need a way to feed the real world temperature fluctuations into that frequency response function to determine the actual structural response. A very natural approach commonly used in structural dynamics consists in determining the temperature fluctuations Power Spectral Density (PSD).

Mathematically, assuming one has a temperature fluctuation record with sampling period T_s, the Discrete Fourier Transform (DFT) of the temperature signal $T(t)$ can be written:

$$DFT(f) = \frac{2}{n_s}\sum_{ind=1}^{n_s} T(ind.T_s)e^{-2i\pi f.ind.T_s} \quad (6)$$

Assuming this operation has been repeated for a number of n_b time blocks each one having duration T_{block}, the PSD will read:

$$\widehat{\Phi}_{TT}(f) = \frac{1}{n_b T_{block}}\sum_{i=1}^{n}|DFT(f,T_{block})|^2 \quad (7)$$

This seemingly cumbersome formula has a very straightforward physical meaning. The quantity $\widehat{\Phi}_{TT}(f)$ would be the mean square amplitude of the original temperature fluctuation after being processed by a (nearly) ideal band-pass filter, with centre frequency f and unitary bandwidth.

Therefore, the total signal energy can be retrieved by summing up all of its components, i.e.:

$$T^2 = \int_0^{f_{maxi}} \widehat{\Phi}_{TT}(f)df \quad (8)$$

Of course, the uppermost frequency (f_{maxi}) is generally not known beforehand and must be selected based on the thermal mechanical susceptibility of the system at hand.

.

[†] The only cases are when day/night cycles dominate, but this is generally the case for non-stabilized cavities.

Application to Stability Analysis

So far, we have developed:

- a tool to break down the real-world (random) temperature fluctuation signal into harmonic components, the PSD
- another tool that can estimate the relative harshness of all those individual components, the Frequency Response Function (FRF)

What we look for ultimately is an evaluation procedure of the actual harshness of the original fluctuation signal. This can be estimated in a very straightforward manner. For example, knowing the input (coolant) temperature (T_c) fluctuation PSD, and the FRF between coolant temperature and structural temperature (H_{TsTc}), as displayed in Fig 2, the output (structural) temperature PSD can be obtained as:

$$\widehat{\Phi}_{T_sT_s}(f) = |H_{TsTc}(f)|^2\widehat{\Phi}_{T_cT_c}(f) \quad (9)$$

And finally, the mean-squared structural temperature fluctuation can be obtained writing:

$$\langle T_s^2\rangle_t = \int_0^{f_{maxi}} \widehat{\Phi}_{T_sT_s}(f)df \quad (10)$$

This method can naturally be applied to any quantity of interest (displacement, angle). In the following, it will be referred to as the "FRF" method.

Real-world Illustration

The previous procedure has been applied to real-world temperature transient, with duration of 4 days. The temperature of the SOLEIL coolant circuit (17°C nominal value) has been recorded. This was performed using a high-resolution Digital Multimeter (DataTranslation model DT9829), with an original sampling rate of 2Hz. Temperature sensors were miniature thermistors (NTC type), with a temperature coefficient of about 4.5%/degC in the working temperature range. The whole setup (see Figure 6) was double checked and total RMS uncertainty (sensors to sensor deviation) was shown to be less 1millidegreeC. The signal was subsequently filtered and decimated to a 5s sampling period, resulting in the time-history shown on Figure 7.

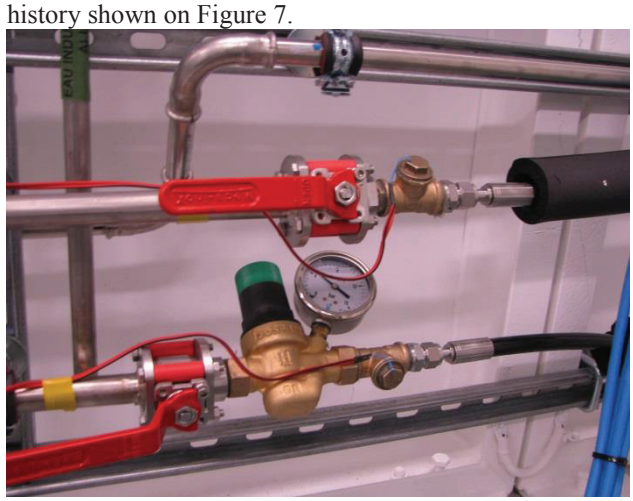

Figure 6 – Coolant water temperature fluctuation measurement (thermal insulation removed).

.

ISBN: 978-3-95450-188-5 doi:10.18429/JACoW-MEDSI2016-TUCA03

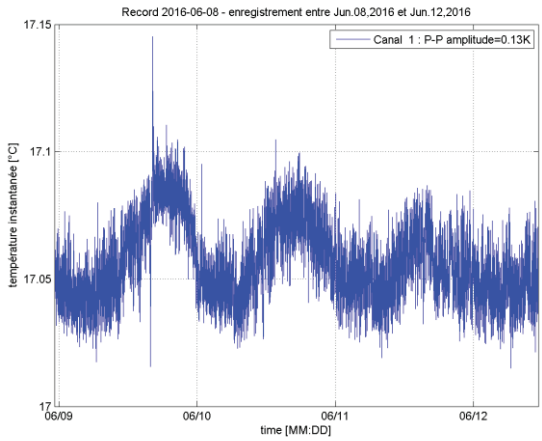

Figure 7: Typical coolant fluid temperature record.

This (purposefully) looks like a well know situation: a dominating quasi-periodic (day/night) component superimposed with a broad band, random noise. This intuition can be consolidated by applying spectral analysis (Figure 8).

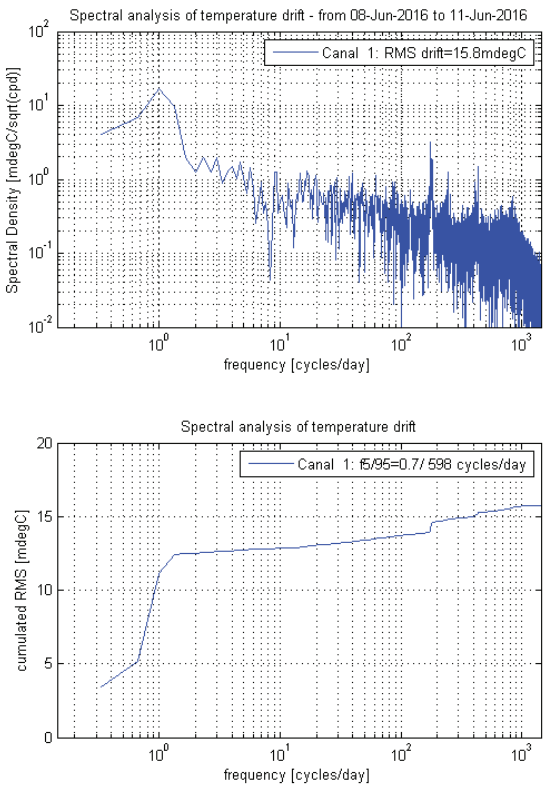

Figure 8: Spectral analysis of coolant fluid temperature.

The uppermost curve represents the square root of the PSD, and has units millidegreeC/sqrt(cycles per day). The lowermost curve is the cumulated RMS level, and provides the RMS amplitude of the signal encompassing all components between 0 (i.e. static) and any frequency. It can be thought of as an indicator of the residual amplitude after applying an ideal low pass filter with variable cut-off frequency *f*.

From the spectral analysis, an interesting fact arises: the cut-off period (700s, equivalent to 123 cycles per day) lies in the far end of the spectrum. The consequence immediately follows: *although we might not expect it, our support structure will statically respond to the coolant temperature fluctuations, with near-zero attenuation due to thermal inertia.*

From an analyst perspective, this is good news, because this means that a simple, quasi static approach is appropriate for the problem at hand.

From a designer perspective, this this is bad news, because this means that one cannot expect any immunity of the structure with respect to coolant-transmitted disturbances.

From an experimentalist point of view, this should also trigger a warning signal, since any extraneous component in the measurements cannot be expected to be efficiently filtered out by the inertia in the thermal mechanical response.

As a means of verification, this simple example was fed into a computer model and a full transient thermal mechanical simulation was executed (Figure 9 and 10). The corresponding spectral contents are compared in Figure 11. This is of course neither practical nor necessary in the engineering practice, but merely aimed at confirming the correctness of our simple approach.

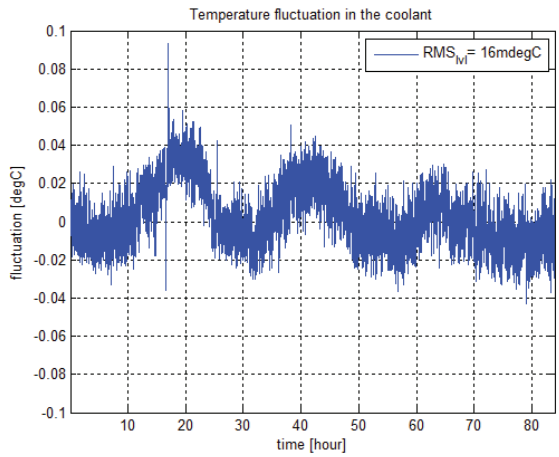

Figure 9: Coolant temperature variations.

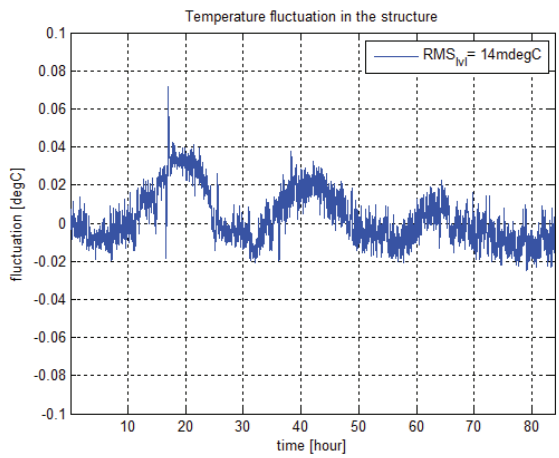

Figure 10: Structural temperature variations.

ISBN: 978-3-95450-188-5 doi:10.18429/JACoW-MEDSI2016-TUCA03

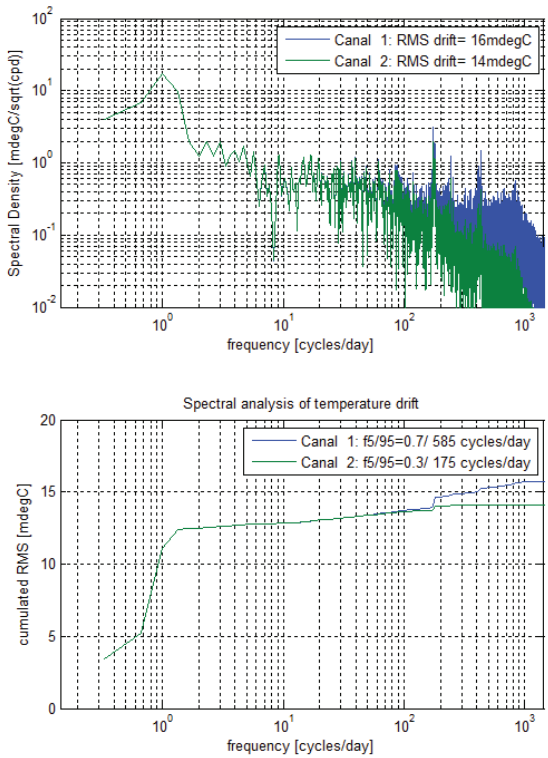

Figure 11: Spectral analysis of coolant/structural temperatures.

We now have confirmation that qualitatively, only minimal temperature attenuation can be expected (14mdegreeC vs 16mdegreeC). The next and more important question is: "does the prediction made using the FRF method also produce reliable estimates regarding position and pointing errors?"

The displacements obtained via detailed FEM analysis are as follows (see Figure 12 and 13).

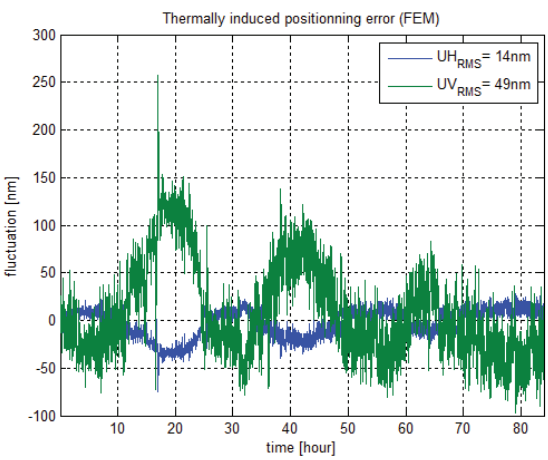

Figure 12: Positioning Error as predicted by FEM transient analysis.

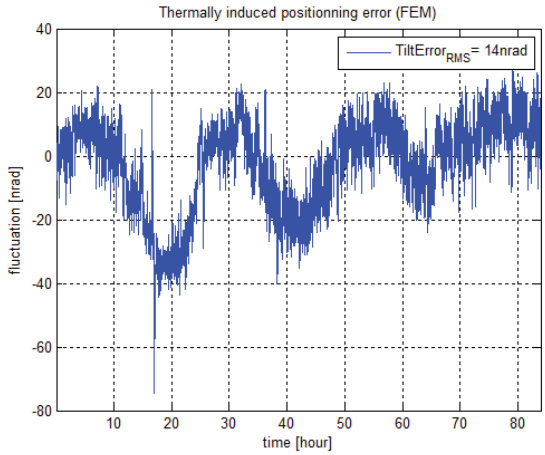

Figure 13: Pointing (Tilt) Error as predicted by FEM transient analysis.

Using the FRF method, very similar results are obtained. The comparison is made in table 1 below:

Table 1: Frequency vs. Time-domain Methods

	Transient	FRF	Ratio
$\mathbf{U_{horizontal}}$	15nm	14nm	0.99
$\mathbf{U_{vertical}}$	50nm	49nm	0.99
$\mathbf{R_{transverse}}$	43nrad	44nrad	1.02

Going a little bit further, we can also compare spectral contents, as shown on Figures 14 to 16:

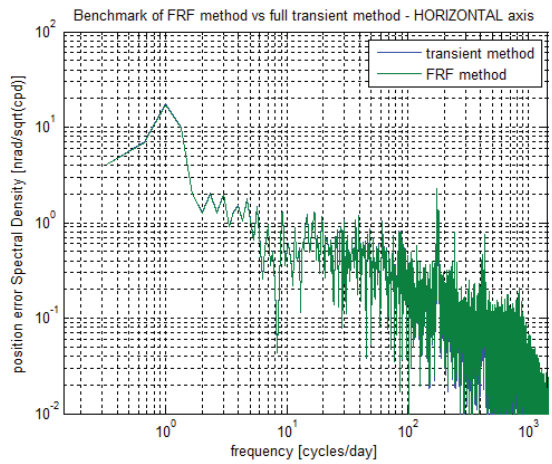

Figure 14: Horizontal Positioning Error as predicted by transient and FRF method.

ISBN: 978-3-95450-188-5 doi:10.18429/JACoW-MEDSI2016-TUCA03

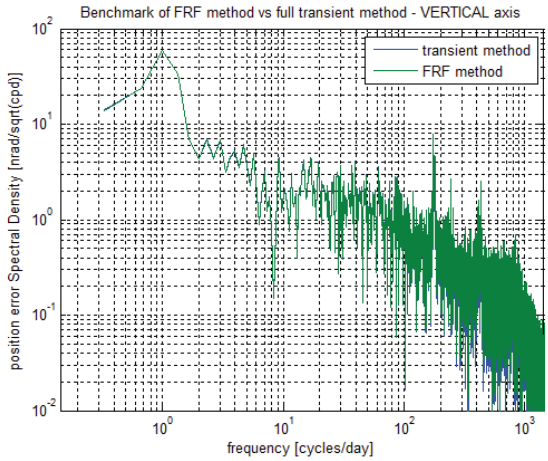

Figure 15: Vertical Positioning Error as predicted by transient and FRF method.

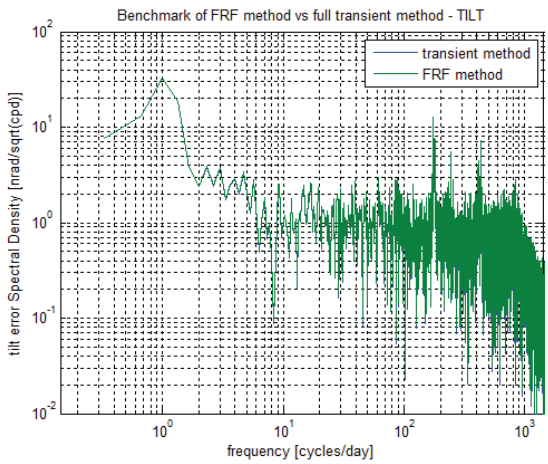

Figure 16: Pointing Error as predicted by transient and FRF method.

As expected, both overall level and the spectra content closely match.

We now have an efficient tool that does provide an accurate estimation of the positioning and pointing errors Root Mean Square (RMS) magnitude and spectral content. This is all very well, but ultimately what is needed from a user's point of view is a probable number of threshold exceedance during an experiment. This will be discussed next.

4 BEAMLINE USER'S PERSPECTIVE: RELIABILITY ANALYSIS

From the user's perspective, the previous considerations are worth listening to, but they lack a fundamental aspect of actual beamline operation that is: time windowing. Since image capturing processes rarely exceed a couple of hours, it is obvious that including the full 24hours drift (for example) in the estimation of the stability clearly induces over-conservatism. Before turning to estimating the stability statistics, we shall therefore take into account the reduction offered by time windowing.

It seems obvious that a simple truncation of the spectra will not do, since low frequency content, albeit attenuated by the finite duration of the observation may still contribute significantly to the total drift. Turning back to the purely harmonic case, it seems obvious that we need to:

- account for the full amplitude of any component whose half period is shorter than the experiment time window
- account for a reduction effect for long term components that capture the worst case scenario, i.e. the experiment takes place at a time (phase) when the drift velocity takes on (and maintains) its peak value.

Assuming a harmonic drifting of amplitude A_{drift} and period T_{drift}, the peak drift rate will read

$$\left(V_{drift}\right)_{peak} = 2\pi \frac{A_{drift}}{T_{drift}}$$

Therefore, the worst-case scenario is that of a steady drift during the whole scanning process, hence effective deviation amplitude reads:

$$A_{effective} = 2\pi \frac{T_{scan}}{T_{drift}} A_{drift}$$

Consequently, we propose to employ the following reduction factor F_{TW} for taking into account the time window effect:

$$F_{TW}\left(\frac{T_d}{T_s}\right) = \frac{2\pi}{Td/Ts + 2\pi}$$

This can be rewritten using frequency instead of period, as illustrated on Figure 17:

$$F_{TW}(f, T_s) = \frac{2\pi}{1/(f \times Ts) + 2\pi}$$

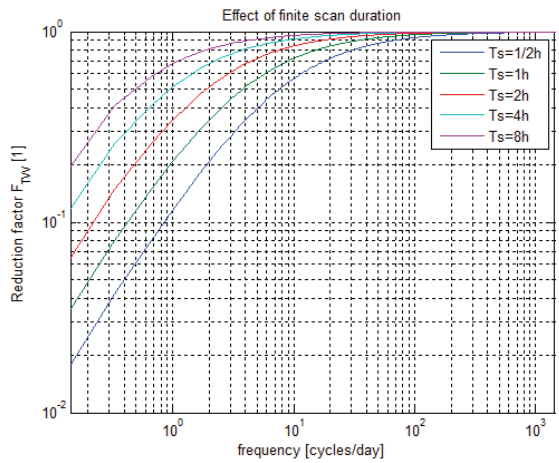

Figure 17: Time Windowing Reduction factors.

Employing this reduction factor yields a substantial reduction in RMS drift amplitude: returning to our test case: we can now estimate the RMS drift amplitudes for various time window durations, as given in Table 2 and graphically displayed in Figure 18 and 19.

ISBN: 978-3-95450-188-5 doi:10.18429/JACoW-MEDSI2016-TUCA03

Table 2: Effect of Time-windowing on RMS Drift

	Ts values [h]					Ref
	1/2	1	2	4	8	inf
U_{hor} [nm]	6	7	8	9	11	15
U_{ver} [nm]	21	24	27	33	37	49
R_{tr} [nrad]	35	36	37	38	40	44

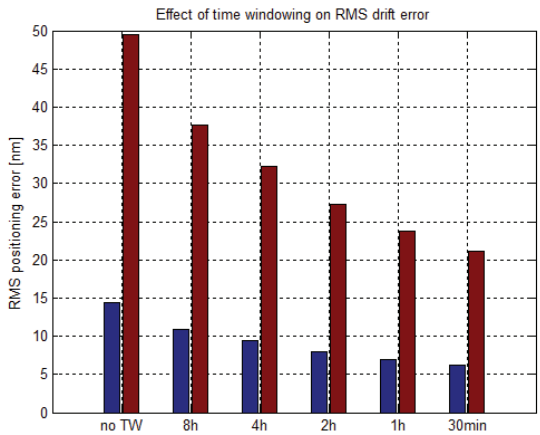

Figure 18: Effect of time windowing on position error.

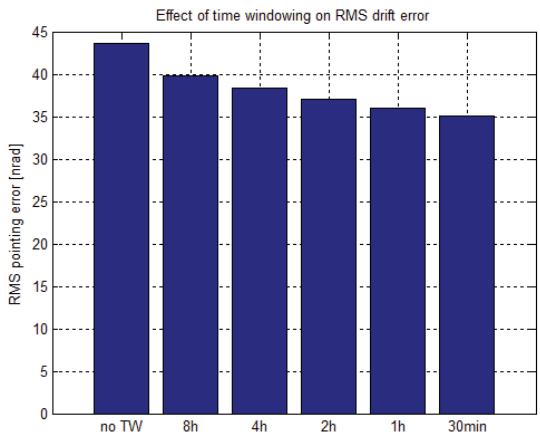

Figure 19: Effect of time windowing on pointing error.

It can be noted that, while the position error is significantly reduced by the time window effect, pointing error almost remains the same. This apparent paradox disappears when examining the frequency content of the pointing error. Pointing errors are dominated by high-frequency components (above 100 cycles/day), hence removing the slow (24h) drift component does not bring much improvement, see Figure 20 to 22:

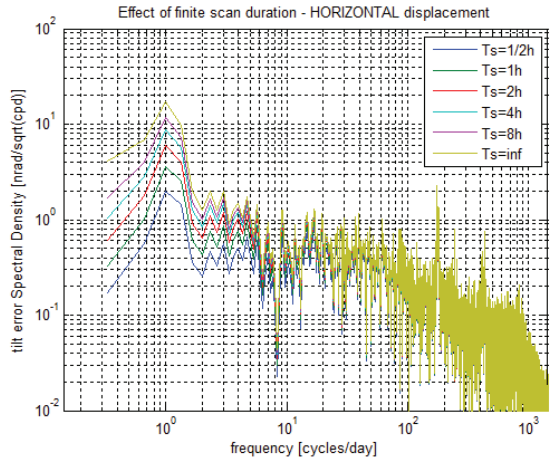

Figure 20: Spectral analysis of VERTICAL drift / Effect of Time Windowing.

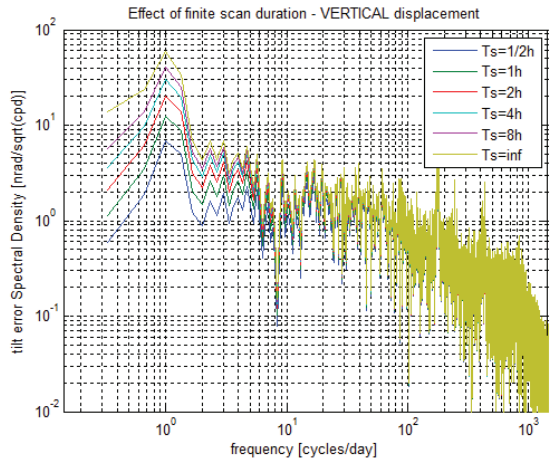

Figure 21: Spectral analysis of VERTICAL drift / Effect of Time Windowing.

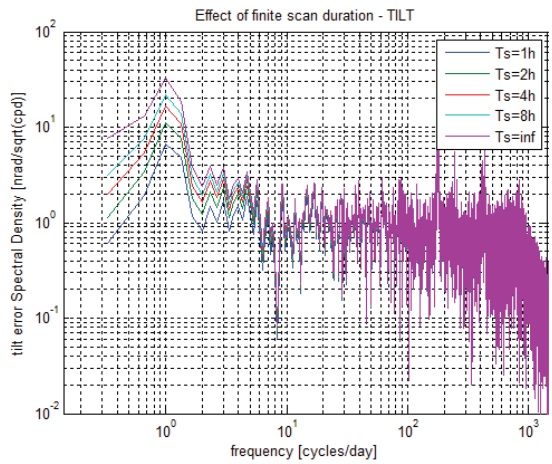

Figure 22: Spectral analysis of TILT drift / Effect of Time Windowing.

Knowing the finite-duration drift RMS levels, we are now in a position to quantify the actual reliability of the mechanical setup. As an example, assuming we have a defined allowable drift threshold *AD* (for example, half a pixel size) that can be used as a boundary between "good" and "faulty" scans. Then, the percentage of faulty scans

ISBN: 978-3-95450-188-5 doi:10.18429/JACoW-MEDSI2016-TUCA03

over an observation window of duration T_s can be conveniently estimated using the conventional formulas for broad[‡] band, stationary Gaussian process.

$$P(|Drift(T_s)| > AD) = 1 - \mathrm{erf}\left(\frac{AD}{\sqrt{2}Drift_{RMS}(Ts)}\right)$$

With:

$$Drift_{RMS}(T_s) = \left(\int_0^{f_{maxi}} F_{TW}(f,T_s)^2 . \left|H_{UT_c}(f)\right|^2 . \widehat{\Phi}_{T_cT_c}(f) df\right)^{1/2}$$

In our case, we can easily estimate the percentage of faulty scans, for various $T_s$values. Following is a numerical simulation assuming a 100nm allowable positioning error along both directions: in that (fictitious) case the percentages of faulty scans would read as follows:

Table 3: Effect of Time-windowing on Reliability ([%] of Faulty Scans).

	Ts values [h]					Ref
	1/2	**1**	**2**	**4**	**8**	**inf**
U_{hor} [nm]	0	0	0	0	0	0.1
U_{ver} [nm]	1.8	3.5	6.7	12.1	18.4	31.2

In this particular case, there is a dramatic decrease in the proportion of the faulty scans when reducing the experiment duration. This conclusion holds whenever there are large components with period longer than the experiments duration.

5 CONCLUSIONS

Through the preceding discussion, we have reached a number of practical conclusions, regarding various perspectives:

- designer (1): high-stability structures are generally small and with high thermal conductivity. Consequently, there is little attenuation of short-period temperature fluctuation to be expected, for both positioning and pointing error, some mild amplification may even occur for the latter. Knowing the working frequency range for temperature stability is essential for drawing sound conclusions.
- analyst (1): it is essential to obtain an accurate and comprehensive probing of the thermal environment. Short period components are often wrongly discarded as being spurious or simply not adequately recorded. In both cases, there is a loss of information and loss of quality in the conclusion reached.
- analyst (2) Working in the frequency domain is a convenient approach for long-period phenomena such as temperature transients. It allows for instant calculations and offers insight into the controlling phenomena. It also offers more flexibility in assessing uncertainties and testing design alternatives.
- user (1): Reliability (in a stationary environment) is strongly dependent on the experiment duration. Most often, for evaluating an environment, working with RMS quantities is a relevant indicator.
- user (2) In temperature controlled situations, shortening the scan period can decrease the percentage of faulty scans by more than one order of magnitude.

Hopefully, this article will provide a basis for a common language between designer, experimentalists, computer aided analyst and beamline user regarding thermal mechanical stability. A well balanced and efficient design can only be reached through collaboration, and this begins with the usage of mutually meaningful notions and dependency rules.

ACKNOWLEDGEMENT

The author would like to acknowledge the discussions with Professor André Preumont (Université Libre de Bruxelles), who (quite unintentionally) sparked the inspiration needed to transfer the techniques of random vibrations from the field of structural dynamics to that of thermal mechanical studies.

The support from the JTRC-project MAXIV-SOLEIL "Nanoprobe" which provided the motivation for a comprehensive analysis of thermal sources in support structures stability is also to be heartily acknowledged.

[‡] Remembering that, contrary to structural dynamics, there is not resonance phenomenon that would result in a narrow band situation.